

The Formation of Pollutants CO/CO₂ in a Steam-Injected Combustor

Masoud Darbandi¹, Majid Ghafourizadeh¹, Gerry E. Schneider²

¹Department of Aerospace Engineering, Centre of Excellence in Aerospace Systems, Sharif University of Technology
P. O. Box 11365-8639, Tehran, Iran

darbandi@sharif.edu; majid.ghafourizadeh@gmail.com

²Department of Mechanical and Mechatronics Engineering, University of Waterloo
Waterloo, Ontario, N2L 3G1, Canada
gerry.schneider@uwaterloo.ca

Abstract - In this paper, different scenarios for steam injection are examined in a combustor to recognize how the formation of CO and CO₂ pollutants will be affected by such circumstances. The scenarios are inspected via numerical simulations of a chosen combustor. First, the numerical procedures need to be verified. So, we simulate the reactive flow in the combustor under the conditions performed in the corresponding experiment. We validate the numerical solutions by comparing the predicted flame structure with the measured ones. The comparison proves that the current simulations predict the profiles of temperature and CO/CO₂ mass fractions sufficiently accurate. So, we take one more step forward and study different scenarios for the steam injection. To the best of our knowledge, there is no study in literature to investigate these scenarios. We simulate the steam-injected combustors and compare the achieved results with those of the original combustor without equipping it with a steam injector. We consider the steam injection in each of oxidizer and fuel stream separately and compare their contours of temperature, CO, and CO₂ mass fractions inside the combustor with each other. Our explorations indicate that the steam injection reduces the flame temperature as well as the concentrations and emissions of pollutants CO and CO₂. These findings can be readily used by the designers seeking new qualitative approaches to control the pollutants emissions from industry burners.

Keywords: CO Pollutant, CO₂ Pollutant, Steam Injection, Combustor, Turbulent Flame.

Nomenclature

B	=	buoyant force
f	=	mixture fraction
f'^2	=	mixture fraction variance
h	=	total enthalpy
n	=	total number of species
p	=	pressure
r	=	radial component in cylindrical coordinates
u	=	radial velocity component
v	=	axial velocity component
z	=	axial component in cylindrical coordinates
R	=	gas constant
T	=	temperature
V	=	velocity vector
W	=	molecular weight
Y	=	mass fraction
ε	=	turbulence dissipation rate
κ	=	turbulence kinetic energy
μ	=	molecular viscosity coefficient
ρ	=	mixture density

Subscripts, Superscripts, and Accents

e	=	effective magnitude
l	=	laminar
m	=	chemical species index counter
t	=	turbulent

1. Introduction

Pollution control has been the main goals in various research topics performed for a decade. Different approaches have been proposed to control different emission in different combustion systems. Among them, the additive approach has attracted the attention of researchers from different perspectives [1-7]. However, there is lack of resources in literature regarding the steam injection in combustors and their effects on CO/CO₂ pollutants. Indeed, there are very limited resources investigating such effects on the resulting pollutants [8-10]. These resources typically discarded the details of combustion such as chemical reactions or reactive flow and so on. On the other hand, literature also shows that there is lack of study for different scenarios of steam injection in combustors. So, these gaps of knowledge need serious attempts and more attention of the related researchers.

In this paper, we intend to investigate the effects of steam injection on pollutants CO and CO₂ and their emission. Hence, we simulate a benchmark combustor with available experimental data. We will compare the flame structure predicted by the current method with the data reported by Dally et al. [11]. The comparison shows that our numerics can predict the distributions of temperature, CO mass fraction, and CO₂ mass fraction inside the flame enough good. The next step, we study the CO/CO₂ pollutants formation under different scenarios of steam injection into the combustor. The scenarios include steam injection into the incoming oxidizer and fuel streams. We change the boundary conditions of the benchmark combustor regarding the contents of water vapour injected to either oxidizer or fuel streams. We simulate these cases (scenarios) and compare the results obtained to the results of benchmark combustor (without steam injection). We compare the distributions of temperature, CO mass fraction, and CO₂ mass fraction inside the combustor. Our findings indicate that the steam injection would change the thermal characteristics of the combustor as well as the pollutants concentrations and their emissions in the exhaust gases.

2. The Governing Equations

In the cylindrical coordinates, the conservation laws for mass, r - and z -momentums are given by

$$\nabla \cdot (\rho \mathbf{V}) + \rho \frac{u}{r} = 0 \quad (1)$$

$$\nabla \cdot (\rho \mathbf{V}u) = -\frac{\partial p}{\partial r} + \nabla \cdot (\mu_e \nabla u) + \mu_e \frac{1}{r} \frac{\partial u}{\partial r} - \mu_e \frac{u}{r^2} \quad (2)$$

$$\nabla \cdot (\rho \mathbf{V}v) = -\frac{\partial p}{\partial z} + \nabla \cdot (\mu_e \nabla v) + \mu_e \frac{1}{r} \frac{\partial v}{\partial r} + \mathbf{B}_z \quad (3)$$

where $\mu_e = \mu_t + \mu_l$ and $\mathbf{B}_z = -\rho g$. The transport equations for turbulence quantities are given by

$$\nabla \cdot (\rho \mathbf{V}k) = \nabla \cdot \left(\frac{\mu_e}{\sigma_k} \nabla k \right) + \frac{\mu_e}{\sigma_k} \frac{1}{r} \frac{\partial k}{\partial r} + G_k - \rho \varepsilon \quad (4)$$

$$\nabla \cdot (\rho \mathbf{V}\varepsilon) = \nabla \cdot \left(\frac{\mu_e}{\sigma_\varepsilon} \nabla \varepsilon \right) + \frac{\mu_e}{\sigma_\varepsilon} \frac{1}{r} \frac{\partial \varepsilon}{\partial r} + \frac{\varepsilon}{k} (c_1 G_k - c_2 \rho \varepsilon) \quad (5)$$

where $G_x = \mu_e \{2[(\partial v / \partial z)^2 + (\partial u / \partial r)^2 + (u / r)^2] + [(\partial v / \partial r) + (\partial u / \partial z)]^2\}$ and $\mu_r = c_d \rho \kappa^2 / \varepsilon$. The constants of turbulence model are modified according to the round jet corrections [12]. For regions near the solid walls, the wall functions are used due to dominant viscous effects there.

For combustion modelling, we use the steady laminar flamelet approach [13-16] in which the laminar flamelets are pre-computed via the detailed kinetic scheme of Qin [17]. The transport equations for the first two moment of mixture fractions are given by

$$\nabla \cdot (\rho \mathbf{V} f) = \nabla \cdot \left(\frac{\mu_e}{\sigma_f} \nabla f \right) + \frac{\mu_e}{\sigma_f} \frac{1}{r} \frac{\partial f}{\partial r} \quad (6)$$

$$\nabla \cdot (\rho \mathbf{V} f''^2) = \nabla \cdot \left(\frac{\mu_e}{\sigma_f} \nabla f''^2 \right) + \frac{\mu_e}{\sigma_f} \frac{1}{r} \frac{\partial f''^2}{\partial r} + c_g \mu_e (\nabla f)^2 - \rho c_\chi \frac{\varepsilon}{\kappa} f''^2 \quad (7)$$

The turbulence-chemistry interaction is regarded using the presumed-shape functions PDFs. The results from the pre-computed laminar flamelets and turbulent statistics are tabulated as a lookup table. The data of this lookup table provide all thermo-chemical quantities of the solution domain during the numerical solution [18].

Assuming a unit Lewis number, the transport equation for the total enthalpy is given by

$$\nabla \cdot (\rho \mathbf{V} h) = \nabla \cdot \left(\frac{\mu_e}{\sigma_h} \nabla h \right) + \frac{\mu_e}{\sigma_h} \frac{1}{r} \frac{\partial h}{\partial r} + q_{rad} \quad (8)$$

The thermal radiation of gaseous mixture is calculated assuming an optically thick flame. Eventually, the mixture density is obtained from the equation of state as $p = \rho R T \sum_{m=1}^n Y_m / W_m$.

3. Computational Method

The authors have already developed a hybrid FVE code [7, 19-27], which uses the advantages of both cell-centred finite-volume FV method and the finite-element FE features. The solution domain is broken into a large number of quadrilateral elements and then each element is divided into four sub-quadrilaterals. All unknown variables are calculated at elements nodes, located at the element vertices. Assembling the four sub-quadrilaterals around a node, the finite volume cells are constructed in which the conservations laws are applied [7, 19-27]. Discretizing the governing equations, we obtain a few systems of linear algebraic equations, i.e. eight equations corresponding to eight unknowns. The element stiffness matrices are derived and assembled properly to construct two sub-global stiffness matrices, corresponding to the fluid dynamics and thermo-chemistry parameters. They are solved iteratively in two stages using the implicit and semi-implicit approaches.

4. The Benchmark Test Case and Validation

As elaborated before, a gaseous methanol turbulent non-premixed flame stabilized on an axisymmetric bluff-body burner is adopted as the benchmark problem. We compare our results against the experimental data to validate our numerical solutions. We implement the experimental conditions of Dally et al. [11] in our calculations. Because of the symmetry of problem, we consider a rectangular solution domain applying the symmetry boundary conditions at the centre line. The computational domain has 0.1 m \times 0.7 m dimensions. The burner has a bluff-body inside with diameter of 50 mm. The fuel nozzle diameter is 3.6 mm. The fuel is the pure gaseous methanol and the oxidizer (dry air) consists of 23.3% oxygen and 76.7% nitrogen (by mass). The fuel nozzle injects the syngas at a speed of 121 m/s into the combustor. The oxidizer, i.e. co-flow air stream, enters the combustor at a speed of 40 m/s. The initial temperatures of fuel and oxidizer are 373 K and 300 K, respectively. Hence, the methanol is evaporated and delivered through a heated line and injected into the combustion chamber.

As a common practice in every computational study, we need to make sure that our numerical results are mesh-independent. In this regard, we examine our numerical results obtained using three different grid resolutions, of 101×701 , 201×1401 , and 401×2801 . We present the distributions of temperature and CO and CO₂ mass fractions at $r=0$. Figure 1 shows the distributions of these quantities for our mesh-independent study. The figure shows that there are very negligible differences in the obtained results if the computational mesh of 201×1401 is refined further. Hence, we choose this grid resolution through the rest of current study. It provides the mesh-independent results.

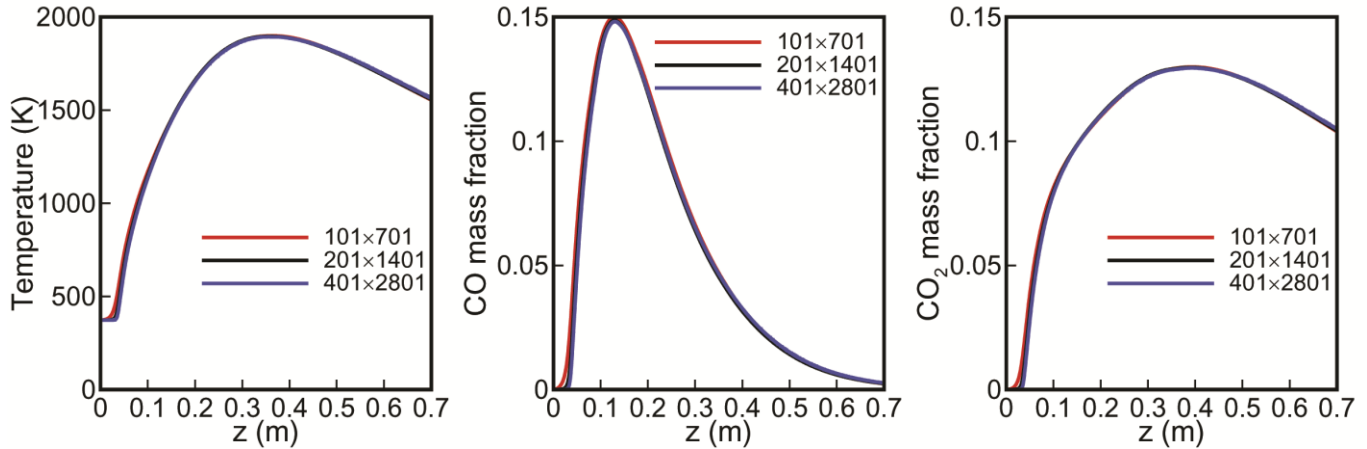


Fig. 1: The distributions of temperature, CO mass fraction, and CO₂ mass fraction at the flame centreline $r=0$ obtained considering different grid resolutions of 101×701 , 201×1401 , and 401×2801 .

To compare the predicted flame structure with those of experiment, Figure 2 shows the distributions of temperature, and CO and CO₂ mass fractions at $z=13, 30, 45, 65, 90,$ and 225 mm in the flame. The distributions are shown using circle symbols. As seen, the black, red, orange, green, blue, and pink colours are used to illustrate the distributions at $z=13, 30, 45, 65, 90,$ and 225 mm, respectively. The distributions are compared with the measured data [11]. The comparison shows that there are great agreements between the obtained results and the experimental data. Of course, there are some discrepancies between them, which can be attributed to the shortcomings of utilized turbulence and radiation models in our simulation. Figure 2 reveals that the current numerical simulation can predict the structure of flame suitably.

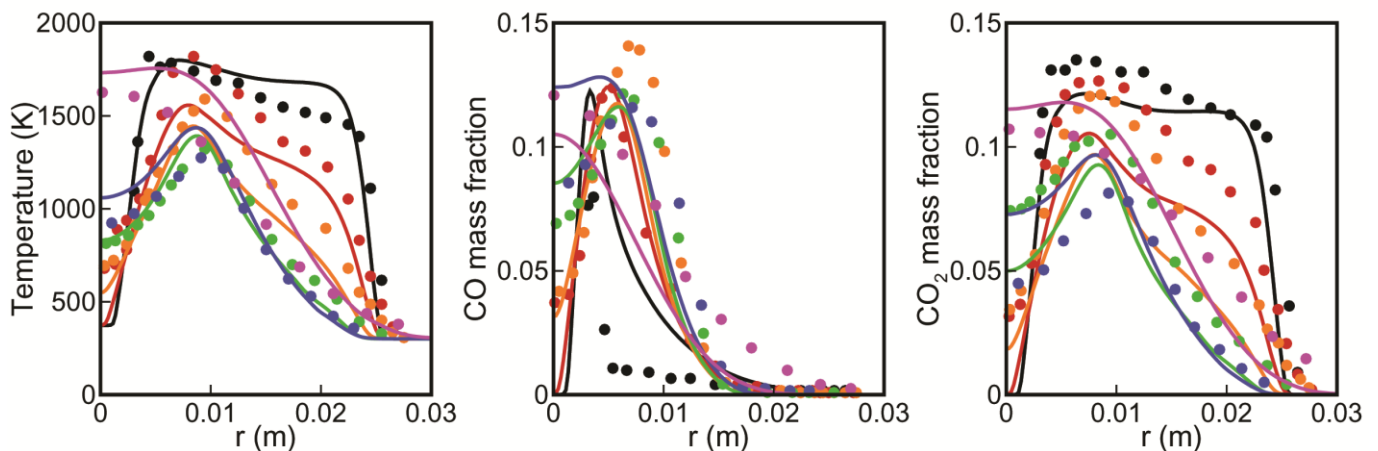


Fig. 2: The distributions of temperature and CO and CO₂ mass fractions and their comparisons with the data reported in experiment of Ref. [11] (symbols); The black, red, orange, green, blue, and pink colours denote the axial locations of $z=13, 30, 45, 65, 90,$ and 225 mm, respectively.

5. Different Scenarios of Steam Injection and its Effects on CO/CO₂ Pollutants

In this section, we would like to study the effects of steam injection on the pollutants CO/CO₂ formation inside the chosen combustor. In this regard, we consider different scenarios of injection including the steam injection in either oxidizer or fuel streams. We change the steam content of these streams separately implementing different boundary conditions for the inlets in the simulation performed above. We change the mass fraction of water vapour from 0 to 0.5 in each of these streams and perform the simulations again. We compare the results obtained for these steam-injected combustor to those of obtained for the original combustor, i.e., the one without steam injection.

Figure 3 presents the distribution of steam mass fraction inside the combustor. The subfigure in left shows the distribution for the combustor without steam injection. The subfigures in middle and right show the distribution for the steam-injected combustors. Indeed, the middle subfigure shows the case of steam-injection in the oxidizer stream of the combustor, whereas the right subfigure shows the case of steam-injection in the fuel stream of combustor.

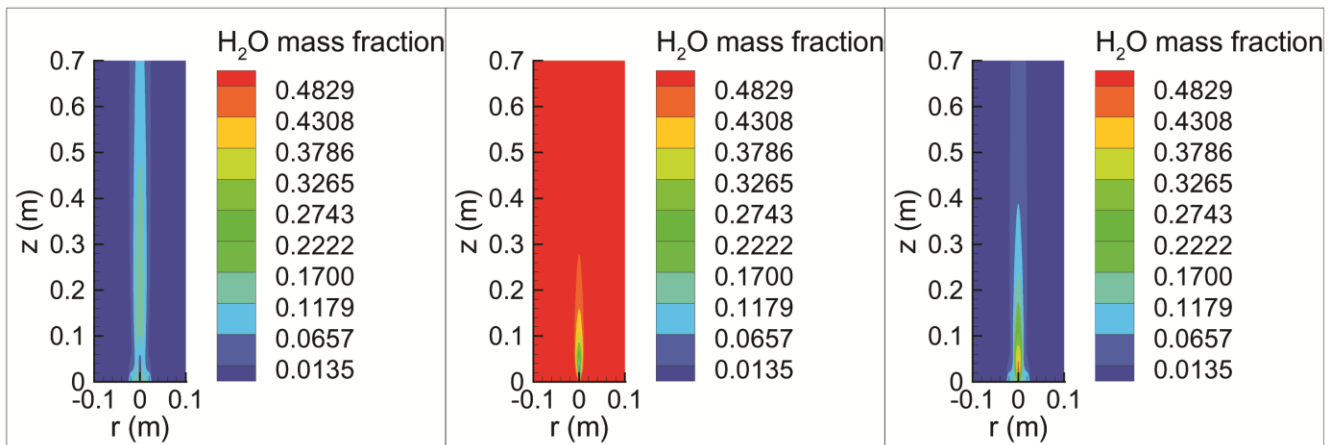


Fig. 3: The distribution of H₂O mass fraction inside the combustor without steam injection (left), with steam injection in the oxidizer stream (middle), and with steam injection in the fuel stream (right).

Figure 4 presents the distribution of temperature inside the combustor. Again, the subfigure in left shows the distribution for the combustor without steam injection. The middle subfigure shows the case of steam-injection in the oxidizer stream, and the right subfigure shows the case of steam-injection in the fuel stream. As observed, the flame temperature decreases as steam is injected into the either oxidizer or fuel stream.

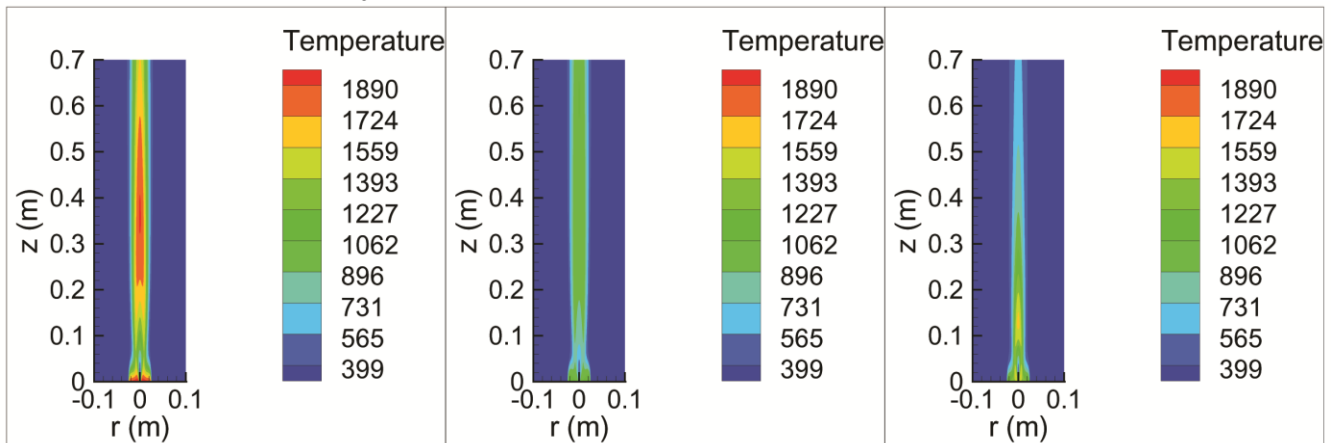


Fig. 4: The distribution of temperature inside the combustor without steam injection (left), with steam injection in the oxidizer stream (middle), and with steam injection in the fuel stream (right).

Figures 5 and 6, respectively, present the distribution of CO mass fraction and CO₂ mass fraction inside the combustor. Same as before, the subfigures in the left column show the distributions for the combustor without steam injection. The subfigures in the middle column show the case of steam-injection in the oxidizer stream, and the subfigures in the right column show the case of steam-injection in the fuel stream. As seen, the concentrations of these pollutants inside as well as their emissions in the exhaust gases reduce when the steam-injection strategy is employed. So, this strategy is a good technique for pollutants reduction in flames and to improve the designs of burners.

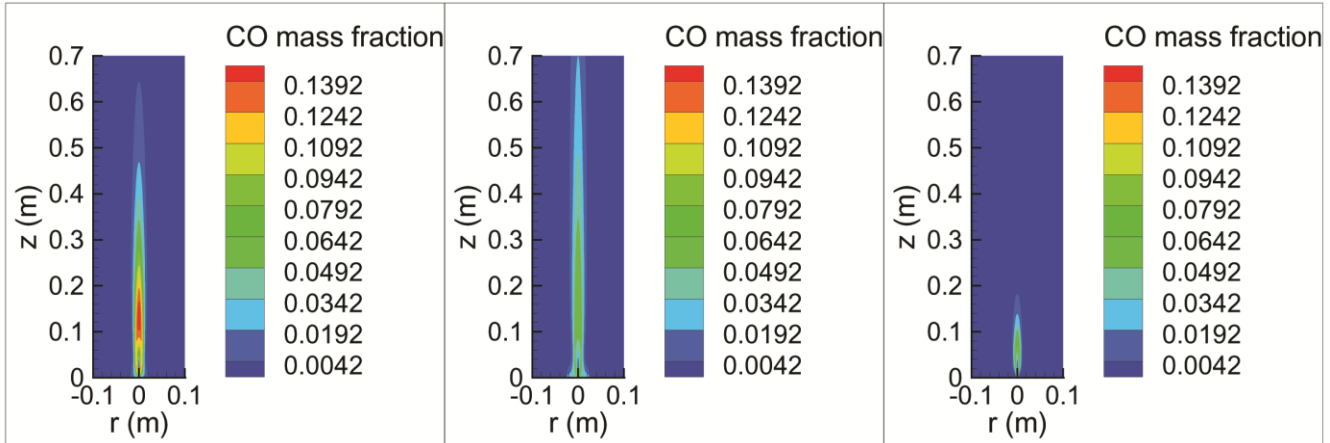


Fig. 5: The distribution of CO mass fraction inside the combustor without steam injection (left), with steam injection in the oxidizer stream (middle), and with steam injection in the fuel stream (right).

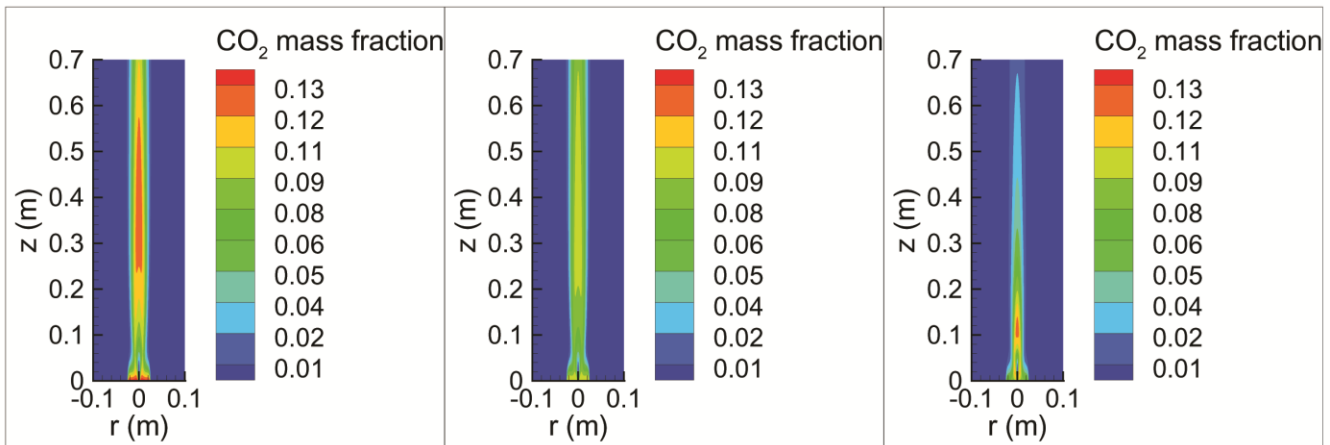


Fig. 6: The distribution of CO₂ mass fraction inside the combustor without steam injection (left), with steam injection in the oxidizer stream (middle), and with steam injection in the fuel stream (right).

6. Conclusion

A steam-injected combustor was simulated to find the impact of injection on the pollutants formation inside the combustor as well as their emissions through the exhaust. Two different scenarios were considered in this study including the steam injection in either oxidizer or fuel stream. At first, the numerical tool was verified focusing on the prediction of flame structure and its comparison with the measurements. Then, the scenarios were carried out by changing the concentrations of water vapour in the two oxidizer and fuel streams. Our findings showed that the flame temperature would decrease as the content of water vapour in the incoming streams was increased. The results indicated that the steam injection could reduce the concentration and emissions of CO and CO₂ pollutants in the combustor and their formations at exhaust considerably.

Acknowledgements

The authors gratefully acknowledge funding from the Deputy of Research and Technology in Sharif University of Technology.

References

- [1] I. Glassman, "Sooting Laminar Diffusion Flames: Effect of Dilution, Additives, Pressure, and Microgravity," *Proceedings of the Combustion Institute*, vol. 27, no. 1, pp. 1589-1596, 1998.
- [2] P. Kumar and D. P. Mishra, "Experimental Study of N₂ Dilution on Bluff-Body Stabilized LPG Jet Diffusion Flame," *Combustion, Explosion, and Shock Waves*, vol. 45, no. 1, pp. 1-7, 2009.
- [3] A. Samanta, R. Ganguly, and A. Datta, "Effect of CO₂ Dilution on Flame Structure and Soot and NO Formations in CH₄-Air Nonpremixed Flames," *Journal of Engineering for Gas Turbines and Power*, vol. 132, no. 12, pp. 124501 (1-5), 2010.
- [4] J. Lee, S. Park, and Y. Kim, "Effects of Fuel-Side Nitrogen Dilution on Structure and NO_x Formation of Turbulent Syngas Non-premixed Jet Flames," *Energy & Fuels*, vol. 26, pp. 3304-3315, 2012.
- [5] R. N. Roy and S. Sreedhara, "A Numerical Study on the Influence of Airstream Dilution and Jet Velocity on NO Emission Characteristics of CH₄ and DME Bluff-Body Flames," *Fuel*, vol. 142, pp. 73-80, 2015.
- [6] F. Liu, A. E. Karatas, O. L. Gulder, and M. Gu, "Numerical and Experimental Study of the Influence of CO₂ and N₂ Dilution on Soot Formation in Laminar Coflow C₂H₄/Air Diffusion Flames at Pressures between 5 and 20 Atm," *Combustion and Flame*, vol. 162, no. 5, pp. 2231-2247, May 2015.
- [7] M. Darbandi, M. Ghafourizadeh, and G. E. Schneider, "The Control of Pollutant Emission from Syngas Flames Using the Oxidizer Dilution Approach," in *4th International Conference of Fluid Flow, Heat and Mass Transfer (FFHMT'17)*, Toronto, Canada, 2017, pp. 107 (1-8).
- [8] M. Renzi, F. Patuzzi, and M. Baratieri, "Syngas Feed of Micro Gas Turbines with Steam Injection: Effects on Performance, Combustion and Pollutants Formation," *Applied Energy*, vol. 206, pp. 697-707, 2017.
- [9] F. Hadia, S. Wadhah, H. Ammar, and O. Ahmed, "Investigation of Combined Effects of Compression Ratio and Steam Injection on Performance, Combustion and Emissions Characteristics of HCCI Engine," *Case Studies in Thermal Engineering*, vol. 10, pp. 262-271, 2017.
- [10] M. Renzi, C. Riolfi, and M. Baratieri, "Influence of the Syngas Feed on the Combustion Process and Performance of a Micro Gas Turbine with Steam Injection," *Energy Procedia*, vol. 105, pp. 1665-1670, 2017.
- [11] B. B. Dally, A. R. Masri, R. S. Barlow, and G. J. Fiechtner, "Instantaneous and Mean Compositional Structure of Bluff-Body Stabilized Nonpremixed Flames," *Combustion and Flame*, vol. 114, pp. 119-148, 1998.
- [12] J. H. Kent and D. Honnery, "Soot and Mixture Fraction in Turbulent Diffusion Flames," *Combustion Science and Technology*, vol. 54, no. 1-6, pp. 383-397, 1987.
- [13] N. Peters, "Laminar Diffusion Flamelet Models in Non-Premixed Turbulent Combustion," *Progress in Energy and Combustion Science*, vol. 10, no. 3, pp. 319-339, 1984.
- [14] D. C. Haworth, M. C. Drake, and R. J. Blint, "Stretched Laminar Flamelet Modeling of a Turbulent Jet Diffusion Flame," *Combustion Science and Technology*, vol. 60, no. 4-6, pp. 287-318, 1988.
- [15] M. Hossain, J. C. Jones, and W. Malalasekera, "Modelling of a Bluff-Body Nonpremixed Flame Using a Coupled Radiation/Flamelet Combustion Model," *Flow, Turbulence and Combustion*, vol. 67, pp. 217-234, 2001.
- [16] R. Prieler, M. Demuth, D. Spoljaric, and C. Hochenauer, "Numerical Investigation of the Steady Flamelet Approach under Different Combustion Environments," *Fuel*, vol. 140, pp. 731-743, 2015.
- [17] Z. Qin, V. V. Lissianski, H. Yang, W. C. Gardiner, S. G. Davis, and H. Wang, "Combustion Chemistry of Propane: A Case Study of Detailed Reaction Mechanism Optimization," *Proceedings of the Combustion Institute*, vol. 28, pp. 1663-1669, 2000.
- [18] E. Sozer *et al.*, "Turbulence-Chemistry Interaction and Heat Transfer Modeling of H₂/O₂ Gaseous Injector Flows," in *48th AIAA Aerospace Sciences Meeting Including the New Horizons Forum and Aerospace Exposition*, Orlando, Florida, 2010, pp. AIAA 2010-1525.

- [19] M. Darbandi, M. Ghafourizadeh, and G. E. Schneider, "A Novel FEV Formulation to Solve Laminar Diffusive Flame in the Cylindrical Coordinates," in *46th AIAA Aerospace Sciences Meeting and Exhibit*, Reno, Nevada, 2008, pp. AIAA 2008-1257: American Institute of Aeronautics and Astronautics, 2008.
- [20] M. Darbandi, M. Ghafourizadeh, and G. E. Schneider, "Numerical Calculation of Turbulent Reacting Flow in a Model Gas-Turbine Combustor," in *41st AIAA Thermophysics Conference*, San Antonio, Texas, 2009, pp. AIAA 2009-3926: American Institute of Aeronautics and Astronautics, 2009.
- [21] M. Darbandi, M. Ghafourizadeh, and G. E. Schneider, "Numerical Simulation of Turbulent Reacting Flow in a Combustion Chamber Using Detailed Chemical Kinetics," in *51st AIAA Aerospace Sciences Meeting including the New Horizons Forum and Aerospace Exposition*, Grapevine (Dallas/Ft. Worth Region), Texas, 2013, pp. AIAA 2013-0710: American Institute of Aeronautics and Astronautics, 2013.
- [22] M. Darbandi and M. Ghafourizadeh, "Extending a Hybrid Finite-Volume-Element Method to Solve Laminar Diffusive Flame," (in English), *Numerical Heat Transfer, Part B: Fundamentals: An International Journal of Computation and Methodology*, vol. 66, no. 2, pp. 181-210, 2014.
- [23] M. Darbandi, M. Ghafourizadeh, and G. E. Schneider, "Finite Element Volume Analysis of Propane Preheated Air Flame Passing through a Minichannel," in *ASME 2014 12th International Conference on Nanochannels, Microchannels, and Minichannels*, Chicago, Illinois, USA, 2014, pp. ICNMM2014-21832, V001T13A002: American Society of Mechanical Engineers, 2014.
- [24] M. Darbandi and M. Ghafourizadeh, "Solving Turbulent Diffusion Flame in Cylindrical Frame Applying an Improved Advective Kinetics Scheme," (in English), *Theoretical and Computational Fluid Dynamics* vol. 29, no. 5-6, pp. 413-431, December 2015.
- [25] M. Darbandi, M. Ghafourizadeh, and G. E. Schneider, "Detailed-Chemistry Modeling of a Bluff-Body Stabilized Methanol/Air Turbulent Nonpremixed Flame Using Finite-Element-Volume Method," in *2nd International Conference on Fluid Flow, Heat and Mass Transfer*, Ottawa, Ontario, Canada, 2015, pp. 154 (1-8), 2015.
- [26] M. Darbandi and M. Ghafourizadeh, "A New Bi-Implicit Finite Volume Element Method for Coupled Systems of Turbulent Flow and Aerosol-Combustion Dynamics," *Journal of Coupled Systems and Multiscale Dynamics*, vol. 4, no. 1, pp. 43-59, 2016.
- [27] M. Ghafourizadeh, M. Darbandi, and G. E. Schneider, "Using Hydrogen Influences to Control the Greenhouse Gas Emissions from Methane-Hydrogen Turbulent Flame," in *3rd International Conference on Fluid Flow, Heat and Mass Transfer (FFHMT'16)*, pp. 166 (1-8), 2016.